Bulgarian Academy of Sciences. Space Research and Technology Institute.
Aerospace Research in Bulgaria. 38, 2026, Sofia

DOI: https://doi.org/10.3897/arb.v38.e24

# INVESTIGATION OF THE CORROSION BEHAVIOR OF B95 (AA7075) ALUMINUM ALLOY REINFORCED WITH NANODIAMOND AND TUNGSTEN AFTER EXPOSURE TO OUTER SPACE

***Anna Bouzekova-Penkova[1], Vanya Dyakova[2], Yoanna Kostova[2], Hristina Spasova[2], Adelina Miteva[1]***

*[1]Space Research and Technology Institute – Bulgarian Academy of Sciences*
*[2]Institute of Metal Science, Equipment and Technologies with Hydro- and Aerodynamics Centre "Acad. A. Balevski" – Bulgarian Academy of Sciences*
*e-mail: a_bouzekova@space.bas.bg, v_diakova@ims.bas.bg*

**Keywords:** *aluminium alloy 7075, corrosion resistance alloy, corrosion behavior alloy*

***Abstract***

*This study investigates the corrosion behavior of aluminum alloy AA7075 (B95), reinforced with 0.1 wt.% nanodiamond powder and tungsten. Two sets of alloy samples were stored for 28 months under different conditions: "reference" – under natural terrestrial conditions, and "space" – in outer space, mounted on the International Space Station (ISS). The corrosion resistance of both sample types was evaluated using gravimetric and electrochemical methods in a 3.5% NaCl solution. Despite similar average corrosion rates (~ 0.06 mm/year), significant differences in the surface corrosion morphology were observed. The „space: samples exhibited deeper pitting and localized corrosion along specific microstructural phases, whereas the „reference" samples demonstrated more uniform surface degradation. Electrochemical tests confirmed enhanced corrosion resistance of the „space" alloy, showing a threefold reduction in corrosion current density and a more positive corrosion potential compared to the "reference" samples. This behavior is attributed to microstructural changes induced by prolonged exposure to outer space, including the formation of a denser protective $Al_2O_3$ layer and the migration of alloying elements (Zn, Cu).*

## Introduction

The safe operation of high-strength aluminum alloys, which are widely used as primary structural materials in the aerospace, marine, and automotive industries, requires accurate data on the corrosion resistance of these alloys under various climatic conditions and in aggressive environments. Maintaining the mechanical properties of aluminum alloys while addressing the challenge of enhancing structural weight efficiency without compromising strength and technological performance is a strategic priority in the development of materials intended for extreme environments, particularly for applications in outer space. To improve mechanical performance, the high-strength aluminum alloy B95 (AA7075) [1–5] was modified with nanodiamond powder [6] and tungsten.

The 7000-series aluminum alloys possess complex chemical compositions. The primary role of alloying elements is to enhance mechanical properties; however, their effects on corrosion resistance vary significantly depending on the type and concentration of the added elements. Zinc has a minimal effect on corrosion resistance, but in 7000-series alloys, its presence in combination with other elements may accelerate corrosion processes [7]. Copper reduces corrosion resistance in high-strength aluminum alloys [8]. The influence of magnesium on corrosion resistance is complex and not exclusively positive [9], whereas manganese typically exerts a slight beneficial effect [10]. Silicon is not a principal alloying element in AA7075, but when present, it may exert a neutral or slightly negative effect on corrosion resistance [11]. Iron decreases corrosion resistance and should be kept at low concentrations to ensure optimal performance in corrosive environments [8].

In various engineering applications, preliminary data on the corrosion behavior of aluminum alloys are essential for material selection and design. The objective of this study is to perform a comparative analysis of the corrosion behavior of aluminum alloy AA7075 (B95), modified with ultrafine diamond powder and tungsten, after 28 months of exposure to two different environments: natural terrestrial conditions and outer space.

## Materials and Methods

### Materials

A material based on the high-strength aluminum alloy AA7075, modified with 0.1 wt.% ultradispersed diamond powder (UDDP) with particle sizes ranging from 4 to 7 nm and tungsten, was investigated (Table 1). The initial raw materials, including aluminum powder, alloying elements, UDDP, and tungsten were homogenized using a planetary ball mill. The resulting mixture was subjected to melting followed by casting. For the purposes of the study, cylindrical specimens with dimensions of ø 6 mm and a height of 6 mm were prepared. The specimens were stored for a period of 28 months under two different environmental conditions. One set, designated as “reference” samples (R), was kept under natural terrestrial conditions, while another set, designated as “space” samples (S), was mounted on the exterior of the Russian module “Zvezda” aboard the International Space Station (ISS) [12]. In space, temperature fluctuations occurred within a broad operational range from −120°C to +150°C every two hours, depending on the position of the ISS. Radiation measurements were conducted using the Radiation Risk Dosimeter Radiometer (R3D)-R2 solid-state detector [13], which was also installed on the exterior of the ISS. The accumulated radiation dose was estimated to be approximately 425 kGy [13–14].

*Table 1. Chemical composition of alloy B95*

| Al [wt. %] | Zn [wt. %] | Mg [wt. %] | Cu [wt. %] | Mn [wt. %] | Cr [wt. %] | Fe [wt. %] | Si [wt. %] | Ti [wt. %] | W+UDDP [wt. %] |
|---|---|---|---|---|---|---|---|---|---|
| 86.3-91 | 5-7 | 1.8-2.8 | 1.4-2 | 0.2-0.6 | 0.1-0.025 | to 0.5 | to 0.5 | to 0.1 | to 0.1 |

The microstructure of both types of samples (R and S) consists of an Al α-solid solution, intermetallic compounds, and several types of structural phases exhibiting Chinese script-like morphology [15]. After exposure to open space, the alloy's microstructure exhibited coarsening. The average size of the Al grains increased from 30.4 nm (prior to exposure) to 36.8 nm (after exposure). Additionally, in the intermetallic $MgZn_2$ phase present in the "reference" sample, isomorphic substitution of zinc with copper cations occurred, leading to the transformation of this phase into $Mg(Zn_{1.98}Cu_{0.02})$, accompanied by an increase in particle size from 15.1 nm to 22 nm [16].

A HIROX 5500 scanning electron microscope (SEM, HIROX Europe, Limonest, France) equipped with a BRUKER EXDS system (BRUKER Co., Berlin, Germany) was used to observe the morphology of the corroded surface after the uniform corrosion tests and electrochemical studies.

**Corrosion tests methods**

*A: Uniform Corrosion Test*

Uniform corrosion tests were performed by continuously immersing "reference" and "space" samples in 3.5% NaCl for 240 hours at 25$^{o}$C in a laboratory thermostat. Before testing, the samples were degreased in acetone and treated in dilute $HNO_3$. The samples were weighed on an analytical balance (KERN ABS-N_ABJ-NM). The corrosion rate (CR) was calculated in mm per year according to ASTM G31 [17]. All CR results obtained are averages of three parallel tests. After the corrosion test, the samples were repeatedly washed with warm distilled water, dried and analysed by scanning electron microscopy (SEM) and energy dispersive X-ray spectroscopy (XEDS).

*B: Linear Polarization Test*

The electrochemical tests were carried out in the 3.5 wt% NaCl solution in a 3-electrode cell at room temperature. The working electrodes with a surface area of 1.0 cm$^2$ are made from the samples investigated. A silver chloride (Ag/AgCl) electrode and a platinum (Pt) plate were used as reference and counter electrodes, respectively. The samples were cleaned with 800 grit sandpaper, degreased with alcohol, treated with dilute $HNO_3$ and dried prior to testing.

Linear polarization was measured vs. stable Eocp over a potential range of ± 10 mV, at a scan rate of 0.1 mV/s. Potentiodynamic curves were recorded at 1 mV/s potential scan rate, starting at 250 mV negative to the stable Eocp.

The electrochemical tests were performed using an Autolab galvanostat-potentiostat model PGSTAT 204 and computer software NOVA 2.1. Corrosion current density ($j_{corr}$), corrosion potential ($E_{corr}$), were obtained from the polarization curves.

## Results and Discussions

The results of the uniform corrosion tests of the "reference" and "space" samples are presented in Fig. 1, Fig. 2 and Fig. 3. The calculated average corrosion rate of the "reference" samples is 0.0600 mm/y, which is close to the average corrosion rate of the "space" samples – 0.0573 mm/y.

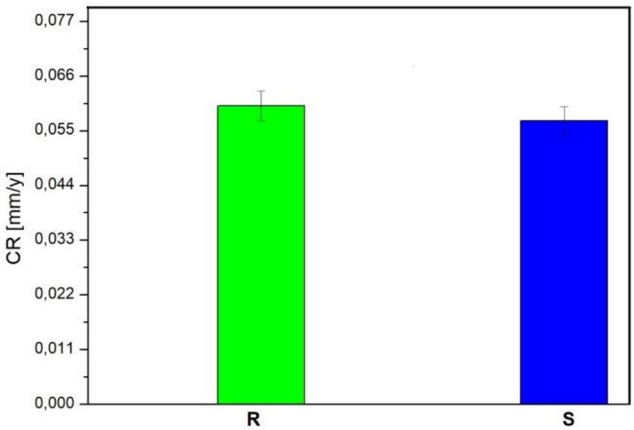


*Fig. 1. Average corrosion rate of "reference" (R) and "space" (S) samples*

Despite the similar average corrosion rates of the two types of samples (R and S) in 3.5% NaCl solution, the nature of the corrosion damage differs, as evidenced by the surface morphology images. The "reference" sample exhibited surface corrosion characterized by areas with scale formation and shallow cracks (Fig. 2a, b), whereas the "space" sample showed wider corrosion ditches and deep pits (Fig. 3a). Energy Dispersive Spectroscopy (EDS) analysis revealed a decreased concentration of aluminum in the ditches and pits, accompanied by elevated levels of copper, manganese, and oxygen within these areas (Fig. 2d and Fig. 3d). The observed differences in corrosion behavior between the two types of samples are attributed to structural changes in the alloy induced by exposure to the outer space environment. Radiation exposure led to the formation of defects in the crystal lattice, facilitating elemental migration particularly of Zn and Cu [16]. Due to temperature fluctuations, these migration processes were accompanied by interdiffusion, resulting in the segregation of aluminum and magnesium oxides, which localized on the surface of the samples [16]. This led to the formation of partially protected regions with limited access to oxygen and aggressive ions from the corrosive medium, thereby promoting corrosion development along the observed Chinese script-like morphology phases (Fig. 3b).

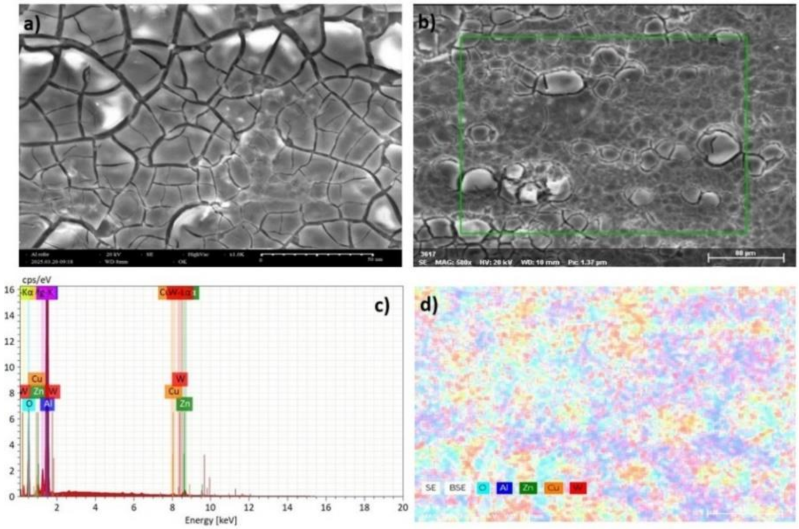


*Fig. 2. Morphology and elemental composition of the surface of the "reference" sample after uniform corrosion test. a) SEM image of the corroded surface, b) Analyzed area, c) EDS spectrum, d) EDS map of the analyzed area*

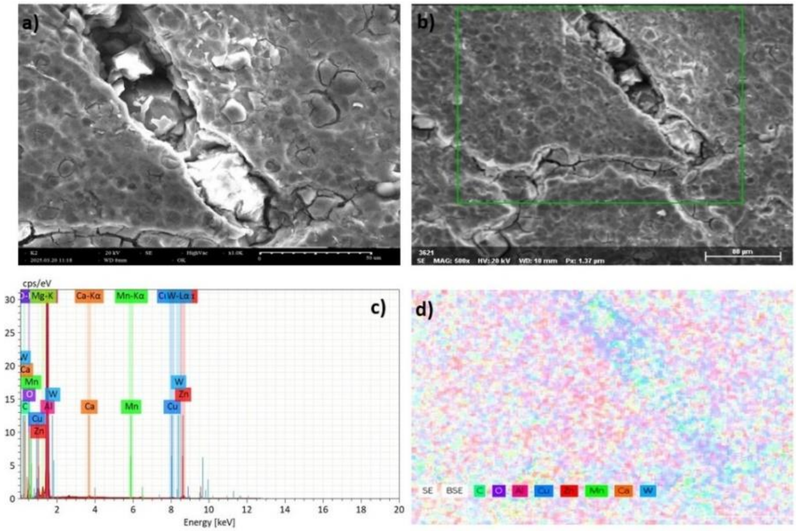


*Fig. 3. Morphology and elemental composition of the surface of the "space" sample after uniform corrosion test. a) SEM image of the corroded surface, b) Analyzed area, c) EDS spectrum, d) EDS map of the analyzed area*

Fig. 4 displays the electrochemical behavior of both sample types (R and S), which shows notable similarities. The linear polarization curves of both the “reference” and “space” samples (Fig. 4) are dominated by the anodic region, corresponding to the dissolution of the aluminum matrix. The anodic curves exhibit multiple fluctuations, likely caused by the formation of a thin hydrated aluminum oxide layer, AlO(OH), during the test [18]. Due to the inhibited anodic dissolution by the denser $Al_2O_3$ layer, the fluctuating anodic region in the “space” sample is shorter, ranging from −0.500 V to +0.600 V (Fig. 4), compared to the “reference” sample. It was established that the AlO(OH) layer predominantly forms in aluminum alloys exposed to terrestrial conditions, while exposure to space conditions favors the formation of a denser, protective $Al_2O_3$ layer, with an $Al_2O_3$:AlO(OH) ratio of approximately 3:1 [16].

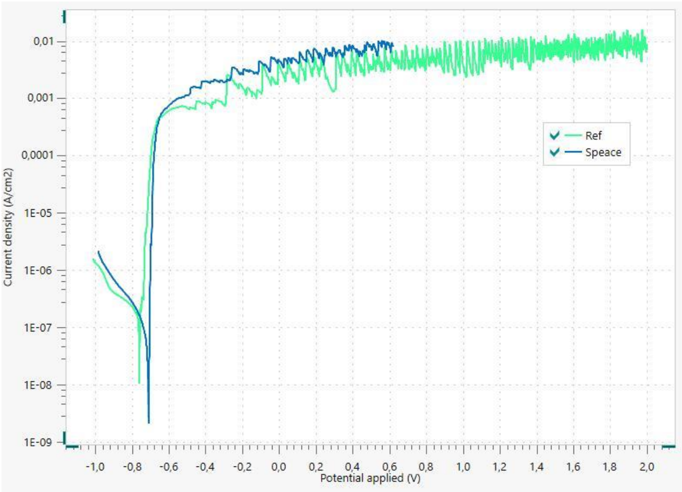


*Fig. 4. Linear polarization curves of “reference” (R) and “space” (S) samples in 3.5 % NaCl solution*

*Table 2. Electrochemical parameters*

| Sample | $i_{corr}$ [A] | $J_{corr}$ [A/cm$^2$] | $E_{corr}$ [V] | CR [mm/y] |
|---|---|---|---|---|
| “Reference” sample (R) | 1.696E-07 | 6.7848E-08 | -0.759 | 0.0022 |
| “Space” sample (S) | 3.064E-08 | 2.188E-08 | -0.724 | 0.0007 |

During the application of electrochemical methods for corrosion testing, real time data on key electrochemical parameters were obtained. The shape of the polarization curves provides both qualitative and quantitative information about the development of the corrosion process, from the moment the specimen is immersed in the electrolyte until the end of the test [19].

The electrochemical parameters recorded during the corrosion tests indicate that the "space" sample exhibits superior anodic protection compared to the "reference" sample. This is evidenced by the corrosion current density ($i_{corr}$) of sample S, which is three times lower than that of R (Table 2). Furthermore, the corrosion potential ($E_{corr}$) of S is more positive than that of R. The corrosion rate of the "reference" sample obtained from electrochemical testing was 0.0022 mm/y, which is higher than the rate for the "space" sample (0.0007 mm/y, Table 2). This difference is attributed to the rapid dissolution of the loosely bound AlO(OH) layer. In contrast, the presence of a dense $Al_2O_3$ layer on the surface of the aluminum matrix in the "space" samples limits the contact with the 3.5% NaCl electrolyte and slows down the corrosion process [16, 17].

Corrosion in both sample types (R and S) primarily initiates at sites where electrochemically active intermetallic cathodic phases such as $MgZn_2$ and $Mg(Zn_{1.98}Cu_{0.02})$ are localized within the anodic aluminum matrix.

Fig. 5 and Fig. 6 present SEM images of the corroded surfaces of the "reference" and "space" samples following the linear polarization test. The "reference" sample shows corrosion distributed across the entire surface (Fig. 5a), whereas in the "space" sample, corrosion is primarily confined to the Chinese script-like morphology phases (Fig. 6a). Fig. 5d and Fig. 6d clearly show the Zn- and Cu-rich areas where corrosion has occurred.

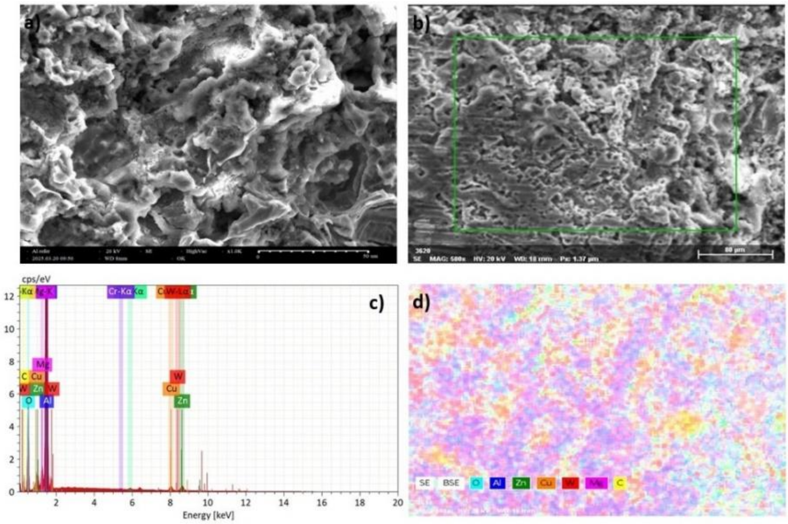


*Fig. 5. Morphology and elemental composition of the „reference" sample (R) after linear polarization. a) SEM image of the corroded surface, b) Analyzed area, c) EDS spectrum, d) EDS map of the analyzed area*

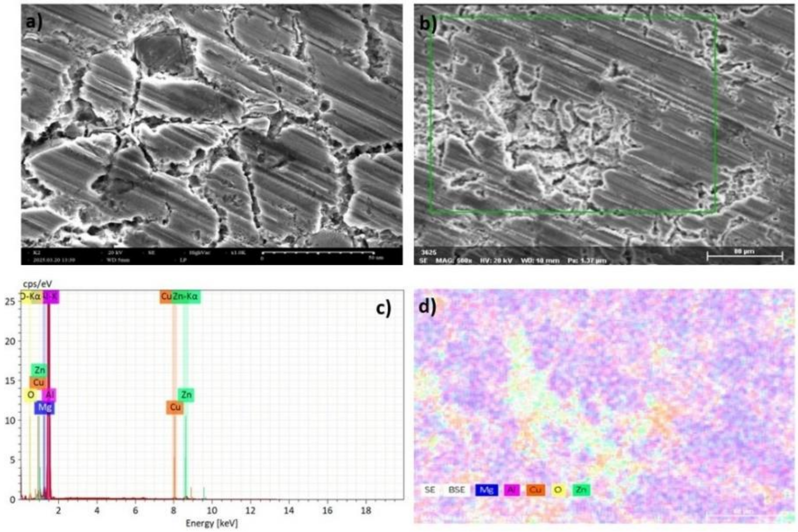

*Fig. 6. Morphology and elemental composition of the "space" sample (S) after linear polarization. a) SEM image of the corroded surface, b) Analyzed area, c) EDS spectrum, d) EDS map of the analyzed area*

## Conclusion

The average corrosion rate of AA7075 alloy samples modified with 0.1 wt.% ultrafine diamond powder and tungsten, which were exposed to terrestrial conditions for 28 months, is 0.060 mm/y, while those exposed to outer space conditions exhibit a rate of 0.057 mm/y. Surface corrosion developed on the "reference" samples, manifested in areas with scales and shallow cracks. In the "space" samples, wider corrosion ditches and pits were observed.

Electrochemical corrosion tests confirmed the results obtained from the general corrosion test and demonstrated better corrosion resistance of the "space" samples. The real-time corrosion rate of the "space" samples is three times lower than that of the "reference" samples, which is attributed to changes in the alloy's microstructure and the migration of Zn and Cu elements during exposure in open space.

These findings suggest that exposure to outer space can beneficially alter the corrosion resistance of advanced aluminum-based composites used in aerospace applications.

## References


1. Fridlyander, I. N. (2002) Modern aluminum and magnesium alloys and composite materials based on them, Metal Science and Heat Treatment. 44, 292–296. https://doi.org/10.1023/A:1021255804324
2. Rambabu, P., Eswara Prasad, N., Kutumbarao, V. V., Wanhill, R. J. H. (2017) Aluminium Alloys for Aerospace Applications. In: Prasad, N., Wanhill, R. (eds) Aerospace

Materials and Material Technologies, Indian Institute of Metals Series, Springer, Singapore. https://doi.org/10.1007/978-981-10-2134-3_2
3. Fridlyander, I. N. (1960) High-strength deformable aluminum alloys, M. Oborongiz, 291. (in Russian)
4. Fridlyander, I. N., Senatorova, O. G., Tkachenko, E. A. (2001) High-strength alloys of the Al–Zn–Mg–Cu system, Mechanical Engineering, Encyclopedia 3, Colored metals and alloys, Moscow, Engineering, 94–128. (in Russian).
5. Fridlyander, I. N. (2002) Aluminum alloys in aircraft in the periods 1970-2000 and 2001–2015, Journal of Light Alloy Technology, 4, 12–17. ISSN 0321-4664 (in Russian)
6. Stavrev, S., Markov L., et. al. (1990) Method for production of ultradispersed diamond, BG patent № 93185/1990. (in Bulgarian)
7. Zongzheng, He, Mingdong, Wu, Shuo, Y., Shuwei, Y., Daihong, X., et. al. (2024) Effect of Zn/Mg ratio on microstructure, mechanical properties and corrosion resistance of 7075 aluminum alloy, Heat Treatment of Metals, 49 (5), 1–9. DOI:10.13251/j.issn.0254-6051.2024.05.001
8. Davis, J. R. (1999) Corrosion of aluminum and aluminum alloys, Asm International. DOI:https://doi.org/10.31399/asm.tb.caaa.9781627082990
9. Haque, M. S., Nomani, M., Akter, A., Ovi, I. A. (2024) Synergistic effect of Mg addition on the enhancement of the mechanical properties and evaluation of corrosion behaviors in 3.5 wt% NaCl of aluminum alloys. Heliyon, 10 (3):e25437. DOI: 10.1016/j.heliyon.2024.e25437
10. Borzooei, R., Azadi, M., Tajally, M., Habibolahzadeh, A. (2025) The effect of manganese on the corrosion properties of Al-Fe alloys in two corrosive solutions, Journal of Alloys and Compounds, 1022, 180018. https://doi.org/10.1016/j.jallcom.2025.180018
11. Oya, Y., Kojima, Y., Hara, N. (2013) Influence of silicon on intergranular corrosion for aluminum alloys. Materials transactions, 54 (7), 1200–1208. https://doi.org/10.2320/matertrans.M2013048
12. Bouzekova-Penkova. A., Klimov, S., Grushin, V., Lapshinova, O., Novikov, D., et. al. (2023) Space Experiment “Obstanovka (1 - stage)”, block DP - PM of the Russian segment of the International Space Station (ISS), Aerospace Research in Bulgaria, 35, 156–164, https://doi.org/10.3897/arb.v35.e15
13. Dachev, T. P., Bankov, N. G., Tomov, B. T., Matviichuk, Yu. N., Dimitrov, P.G. et al. (2017) Overview of the ISS radiation environment observed during the ESA EXPOSE-R2 mission in 2014-2016, Space Weather, 15 (11), 1475–1489. https://doi.org/10.1002/2016SW001580
14. https://cosmicrays.oulu.fi/ (April 10, 2025)
15. Bouzekova-Penkova, A., Simeonova, S., Dimitrova, R., Dimitrova. R. (2020) Structural properties of aluminium alloy enhanced by nanodiamond and tungsten exposed in the outer space, Comptes rendus de l’Acade'mie bulgare des Sciences, 73 (9), 1270–1276. DOI:10.7546/CRABS.2020.09.11
16. Bouzekova-Penkova, A., Tzvetkov, P. (2019) Investigation of outer space influence on structural properties of strengthened 7075 aluminum alloy. Experiments onboard the international space station (ISS), Comptes rendus de l’Acade'mie bulgare des Sciences, 72 (7), 939–946. DOI: 10.7546/CRABS.2019.07.12

17. Kucuk, İ. (2018) Effect of Cold Rolling Reduction Rate on Corrosion Behaviour of Twin-roll Cast 8006 Aluminium Alloys, Cumhuriyet Science Journal, 39 (1), 233–242. https://doi.org/10.17776/csj.390178
18. Bagherzadeh, M., Karimi, M., Choopan Dastjerdi, M. H. C., Asadabad, M. A., Mokhtari, J., et.al. (2023) Long-time irradiation effect on corrosion behavior of aluminum alloy in pool water of low-power research reactor, Scientific Reports, 13, 17007. https://doi.org/10.1038/s41598-023-44287-0
19. Esmaily, M., Svensson, J. E., Fajardo, S., Birbilis, N., Frankel, G. S., et. al. (2017) Fundamentals and advances in magnesium alloy corrosion. Progress in Materials Science, 89, 92–193. https://doi.org/10.1016/j.pmatsci.2017.04.011

## ИЗСЛЕДВАНЕ НА КОРОЗИОННОТО ПОВЕДЕНИЕ НА АЛУМИНИЕВА СПЛАВ В95 (7075) УЯКЧЕНА С НАНОДИАМАНТ И ВОЛФРАМ СЛЕД ПРЕСТОЙ В ОТКРИТИЯ КОСМОС

*А. Бузекова-Пенкова, В. Дякова, Й. Костова,*
*Х. Спасова, А. Митева*

**Резюме**

Това проучване изследва корозионното поведение на алуминиева сплав AA7075 (B95), подсилена с 0,1 wt.% нанодиамант на прах и волфрам. Два комплекта образци от сплавта бяха съхранявани 28 месеца при различни условия: “референтни” – при естествени земни условия и “космически” – в откритият космос, монтирани на борда на Международната космическа станция (МКС). Устойчивостта на корозия на двата типа образци беше оценена чрез гравиметрични и електрохимични тестове в 3,5% разтвор на NaCl. Въпреки сходните средни скорости на корозия (~ 0,06 mm/y), се наблюдават значителни разлики в морфологията на корозиралата повърхност. „Космическите“ образци показват по-дълбоки питинги и локализирана корозия, по специфични микроструктурни фази, докато “референтните” образци показват по-равномерно разграждане на повърхността. Електрохимичните тестове потвърдиха повишена устойчивост на корозия в изложената в космоса сплав, с плътност на корозионния ток три пъти по-ниска и по-положителен корозионен потенциал от този на “референтните” образци. Това поведение се дължи на индуцирани от престоя в открития космос микроструктурни промени на сплавта, включително образуването на по-плътен защитен слой $Al_2O_3$ и миграция на елементи (Zn, Cu).